Journal of Power Sources 195 (2010) 2414–2418

Contents lists available at ScienceDirect

Journal of Power Sources

journal homepage: www.elsevier.com/locate/jpowsour

Short communication

Polymer/graphite oxide composites as high-performance materials for electric double layer capacitors

Chien-Pin Tien, Hsisheng Teng*

Department of Chemical Engineering and Center for Micro/Nano Science and Technology, National Cheng Kung University, No. 1 Ta-Hsueh Road, Tainan 70101, Taiwan

ARTICLE INFO

Article history:
Received 25 April 2009
Received in revised form
29 September 2009
Accepted 2 November 2009
Available online 6 November 2009

Keywords:
Graphite oxide
Graphene
Polymer incorporation
Electric double layer capacitor
Gel electrolyte

ABSTRACT

A single graphene sheet represents a carbon material with the highest surface area available to accommodating molecules or ions for physical and chemical interactions. Here we demonstrate in an electric double layer capacitor the outstanding performance of graphite oxide for providing a platform for double layer formation. Graphite oxide is generally the intermediate compound for obtaining separated graphene sheets. Instead of reduction with hydrazine, we incorporate graphite oxide with a poly(ethylene oxide)-based polymer and anchor the graphene oxide sheets with poly(propylene oxide) diamines. This polymer/graphite oxide composite shows in a "dry" gel-electrolyte system a double layer capacitance as high as 130 F g^{-1}. The polymer incorporation developed here can significantly diversify the application of graphene-based materials in energy storage devices.

1. Introduction

Electrical double layer capacitors (EDLCs) represent an essential accessory to rechargeable batteries or fuel cells for high power applications such as portable electronic devices and electric vehicles [1–3]. The capacitance in EDLCs is purely electrostatic in origin due to the separation of electron and ionic charges across the electrode/electrolyte interface [4]. To have high specific capacitance, electrodes of EDLCs are generally composed of porous carbon materials having a high surface area and low cost [5–11], such as activated carbon powders and activated carbon fibers. However, a space constriction for charge accommodation, especially inside micropores, limits the proportional increase of capacitance with the surface area [12,13]. Micropores of activated carbon have been suggested to be ideally slit-shaped due to the fact that activated carbon is composed of graphitic crystallites [14,15]. Etching the wall of the slit-shaped pores can be a solution to remove the space constriction [16]. Alternatively, exfoliation of graphite powders can also provide a carbon material having a minimum space constriction [17]. Another important challenge for EDLCs is the use of gel electrolytes to avoid solvent leakage or evaporation, which limits the long-term stability of the EDLCs [5]. However, the pores of activated carbon are not accessible to the polymer chains of the gel electrolytes [18–21]. This limits the solvent-entrapping ability of the polymer framework in the EDLC system. Under this circumstance, an exfoliated graphite structure becomes an ideal carbon form not only to accommodate electrolyte ions for double layer formation, but also to allow thorough penetration of polymer chains [22–24]. The present work demonstrates how exfoliated graphite oxides, without reduction with hydrazine [25–27], can be employed to fabricate high-capacitance EDLCs assembled with a gelled polymer electrolyte.

The graphite lattice has been exfoliated via chemical oxidation to disrupt the weak van der Waals forces, allowing for easy penetration with molecules. This process results in formation of graphite oxide, of which the interlayer space is occupied by epoxy, hydroxyl and carbonyl functionalities [28,29]. The functional groups can be obstacles for electrolyte motion between the graphene sheets. To promote electrolyte ion transport, we incorporate graphite oxide with poly(ethylene oxide) (PEO)-based polymer to increase the interlayer spacing as well as to convey the electrolyte ions through the segmental motion of the polymer chains [20,21]. This polymer/graphite oxide composite can also be coupled with a gel-electrolyte film made of the same PEO-based polymer to avoid solvent leakage, assuring long-term stability of an EDLC system.

Another advantage of polymer incorporation is that the use of high-crystallinity graphite for graphene sheet separation would not be essentially necessary. The degree of exfoliation depends on the crystallinity of the precursor graphite used [30]. The high cost of high-crystallinity graphite would hamper the use of exfoliated graphite as the electrode materials for EDLCs. With polymer incorporation, the graphite oxide with their interlayer spacing

* Corresponding author. Tel.: +886 6 2385371; fax: +886 6 2344496.
E-mail address: hteng@mail.ncku.edu.tw (H. Teng).

0378-7753/$ – see front matter © 2009 Elsevier B.V. All rights reserved.
doi:10.1016/j.jpowsour.2009.11.001

expanded can be used as an efficient electrode material for EDLCs alternative to the separated graphene sheets [17]. In the present work, we obtain polymer/graphite oxide composites by using low-crystallinity graphite as the precursor.

To synthesize the polymer host for the gel electrolyte, a poly(ethylene oxide)-*co*-poly(propylene oxide) network, designated as P(EO-*co*-PO), is prepared from poly(ethylene glycol) diglycidyl ether (PEGDE) with poly(propylene oxide) diamines used as the curing agent [20]. Diglycidyl ether of bisphenol-A (DGEBA) is also blended with the polymer precursors before curing to enhance the mechanical properties. The chemical structures of the polymer precursors and the resulting polymer network have been reported elsewhere [20]. The addition of poly(propylene oxide) to the PEO network can promote the mechanical properties as well as the ion-conveying ability. A form of polymer/graphite oxide composite can be obtained by mixing graphite oxide with the polymer precursors and subsequently heating the mixture for polymerization. This composite can be readily incorporated into EDLCs for test. Here, we demonstrate that this polymer/graphite oxide composite is superior to porous carbons in electric double-layer charge storage when it is used to assemble a gel-based "dry" supercapacitor.

2. Experimental

Graphite oxide was synthesized from a low-purity natural graphite powder (Kanto, Japan) by using the Hummers–Offeman method [29,31]. The graphite powder (5 g) and $NaNO_3$ (2.5 g; Merck, Germany) were introduced to concentrated H_2SO_4 (18 M, 115 mL; Wako, Japan) in an ice-bath. $KMnO_4$ (15 g; J.T. Baker, USA) was added gradually with stirring, so that the temperature of the mixture was not allowed to exceed 20 °C. The mixture was then stirred at 35 °C for 30 min. At the end of 30 min, de-ionized water (250 mL) was slowly added to the mixture, followed by stirring the mixture at 98 °C for 15 min. The reaction was terminated by addition of 750 mL of 2 wt% H_2O_2 with stirring at 10 °C. Multiple washings with de-ionized water (6× 700 mL) and centrifugations were conducted until the final slurry reaching a neutral pH. The graphite oxide specimen (GO) was obtained by vacuum-drying at 120 °C for 24 h the precipitate of the final slurry. The sonicated GO was obtained from the final slurry with sonication (using an ultrasonic bath cleaner of 400 W) for 1 h.

The P(EO-*co*-PO) polymer was synthesized using PEGDE (Kyoeisha, Japan) and DGEBA (Nan-Ya, Taiwan) with epoxy group equivalent weights of 290 and 190 g(equiv.)$^{-1}$, respectively, and a curing agent, α,ω-diamino poly(propylene oxide) (Huntsman Jeffamine D2000, USA), with an active hydrogen equivalent weight of 514 g(equiv.)$^{-1}$. We prepared the precursor solution of P(EO-*co*-PO) by dissolving 0.1 g PEGDE, 0.1 g DGEBA and 0.45 g Jeffamine D2000 in 0.5 g acetone.

To prepare a polymer/graphite oxide composite (*p*GO) as the material for EDLC electrodes, 0.046 g of the sonicated GO was put together with 0.02 g of the P(EO-*co*-PO) precursor solution and 0.2 g acetone and the mixture was sonicated for 10 min to reach homogeneity. After evaporation of acetone, an appropriate amount of the mixture (~4 mg) was spread on a stainless-steel foil of 1 cm^2 in area. With a treatment at 120 °C for 24 h under vacuum, a *p*GO electrode was obtained. The bulk density of *p*GO is 0.995 g cm^{-3}. A commercially available activated carbon (AC; Calgon Filtrasorb 300, USA) was also used to serve as the carbon material for EDLCs. To prepare an electrode, a mixture (~4 mg) of AC and a polytetrafluoroethylene binder (20/1 in weight ratio) was also spread on a stainless-steel foil, followed by drying at 120 °C for 8 h under vacuum.

A symmetric two-electrode capacitor cell was fabricated to examine the capacitive performance of electrodes in a cell. For liquid-phase experiments, the cell was assembled with two facing electrodes, sandwiching a piece of cellulose paper (~30 μm in thickness) as the separator. A solution of 1 M tetraethylammonium tetrafluoroborate ($TEABF_4$; Fluka, UK) in propylene carbonate (PC; Fluka, Germany) served as the liquid electrolyte. In the gel-electrolyte cell, a P(EO-*co*-PO) thin film was used as a separator instead of cellulose paper. The thin film (~30 μm in thickness) was obtained by spreading the P(EO-*co*-PO) precursor onto an aluminum plate with subsequent curing at 120 °C for 24 h under vacuum. Prior to the cell assembly, the film and *p*GO electrodes were soaked in the 1 M $TEABF_4$/PC solution to entrap an appropriate amount of the solution.

Cyclic voltammetric measurements were conducted within −1.5 and 1.5 V at different sweep rates (5–100 mV s^{-1}). The specific capacitance based on per unit AC or GO mass was calculated using integration of the voltammograms within the potential range applied. Single-electrode capacitance is reported in the present work. AC impedance spectroscopic analysis of the *p*GO EDLC cells was conducted at 0 V with an amplitude of 5 mV, while the frequency ranged between 2 mHz and 100 kHz.

Powder X-ray diffraction (XRD) patterns of the carbon materials were obtained by using a Rigaku RINT2000 equipped with Cu Kα radiation (Japan). Scanning electron microscope (SEM) images were obtained with a JOEL JSM-6700F (Japan). Transmission electron microscope (TEM) images were taken on a Hitachi H-7500 (Japan). Fourier transform infrared (FT-IR) spectroscopic analysis in diffuse reflectance mode (DRIFT) was conducted by using a ThermoNicolet 5700 spectrometer. 20 mg of a dry specimen was mixed with 450 mg of finely ground dry KBr (Aldrich, USA) and purged in the sample holder for 60 min by a continuous flow of dry air prior to the analysis. Surface area measurement was conducted using an adsorption apparatus (Micromeritics ASAP2010, USA).

3. Results and discussion

The XRD patterns of the precursor graphite and resulting GO are shown in Fig. 1. The peak positions of the (0 0 2) planes are located at 2θ values of 26.5° and 10.2° for the precursor graphite and GO, respectively. The peak shift indicates that interlayer spacing was expanded by the chemical oxidation from 0.336 to 0.868 nm. After sonication treatment, the GO specimen was exfoliated, as reflected by the disappearance of the diffraction peak (Fig. 1c). Fig. 2a shows the SEM image of the sonicated GO, which is composed of exfoliated graphene oxide layers. Fig. 2b shows the TEM image of the

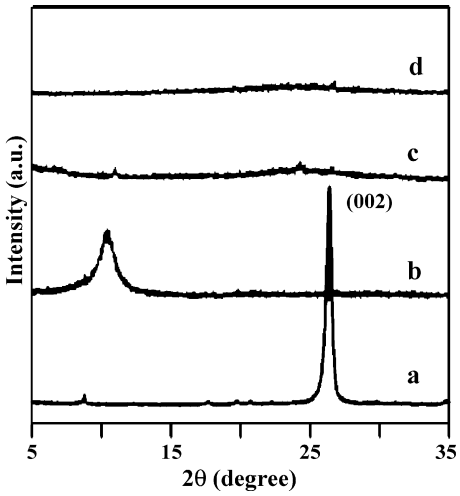

Fig. 1. X-ray diffraction patterns: (a) the precursor graphite; (b) the graphite oxide prior to sonication; (c) the sonicated graphite oxide; (d) the polymer/graphite oxide composite.

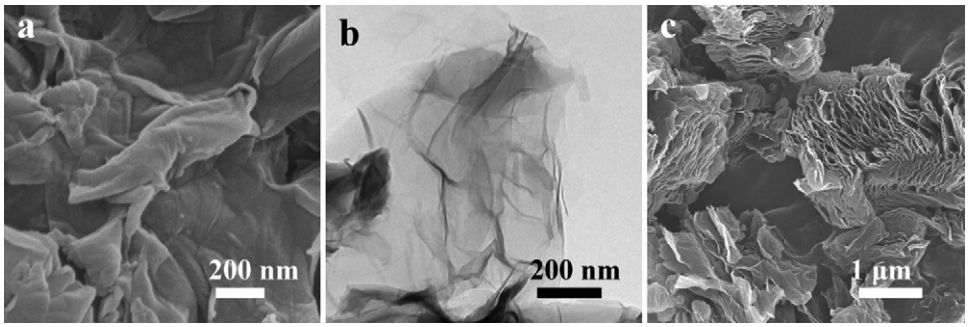

Fig. 2. (a) SEM image of the sonicated graphite oxide; (b) TEM image of some individual graphene oxide sheets extending from the sonicated graphite oxide; (c) SEM image of the polymer/graphite oxide composite.

some individual graphene oxide sheets extending from the bulk of the sonicated GO. These sheets can serve as the electrical contact to bridge the GO aggregates when they are incorporated into EDLC electrodes. The GO obtained from the vacuum-drying at 120 °C was conductive. This aspect will be discussed later. The main body of the sonicated GO is composed of the stacked graphene oxide sheets. Preliminary electrochemical experiments have shown that the capacitive performance of this sonicated GO in organic electrolytes was inferior to *p*GO. Nitrogen adsorption analysis on the sonicated GO showed a BET (Brunauer–Emmett–Teller) surface area as low as 8 $m^2 g^{-1}$. This indicates that the graphene oxide sheets are tightly stacked because of the hydrogen-bonding attraction resulting from the oxygen-containing groups occupying the interlayer space [32]. Both the oxygen-containing groups and strongly adsorbed water molecules (see following discussion) can obstruct the passage of N_2 or electrolytes into the interlayer space.

The rich surface chemistry of the GO specimen was analyzed by FT-IR spectroscopy using KBr pellets, with the spectrometer operating in diffuse reflectance mode. The FT-IR results are shown in Fig. 3. By contrast, no obvious absorbance is observed for the precursor graphite (Fig. 3a). For the sonicated GO (Fig. 3b), the most characteristic features are the intense bands at 900 cm^{-1} (epoxy stretching vibrations), 1100 cm^{-1} (C–O stretching vibrations), and 1230 cm^{-1} (C–OH stretching vibrations) [33–35]. The band of C=O stretching motions near 1720 cm^{-1} is negligible [24,36]. This indicates the functional groups formed from the chemical oxidation on the graphene sheets are mainly in the forms of epoxy bridges C–O–C and phenols –OH. The broad absorption at 3000–3600 cm^{-1} for O–H stretching vibrations is partially due to liquid water since the H–O–H bending band of the H_2O molecules can be observed at 1650 cm^{-1} [35]. It was reported that complete removal of water from GO is practically impossible [36].

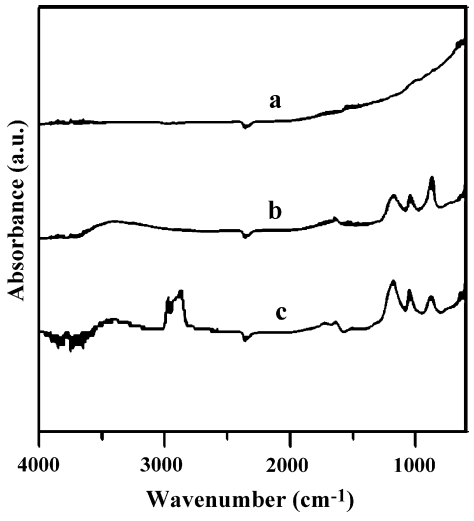

Fig. 3. FT-IR absorbance spectra: (a) the precursor graphite; (b) the sonicated graphite oxide; (c) the polymer/graphite oxide composite.

The *p*GO synthesis was initiated by mixing the polymer precursors and sonicated graphite oxide in acetone. Because of the polar feature of acetone, the interlayer spacing distance can be temporarily extended via acetone penetration [35], which subsequently leads to the penetration of the polymer precursors. Following this temporary penetration, permanent segregation of the graphite oxide can be achieved by an anchoring reaction between the epoxy groups and the poly(propylene oxide) diamines that are also used as the curing agent [22]. The possible reaction scheme is presented in Fig. 4, which shows that the anchoring proceeds with nucleophilic substitution on the epoxy bridges to form graphene–N bonds and –OH groups [22]. Polymerization as well as the anchoring reaction was conducted by heating the polymer precursor-incorporated graphite oxide at 120 °C under vacuum. Fig. 3 shows that there is an obvious emergence of methylene C–H stretching band at 2800–3000 cm^{-1} after the graphite oxide being incorporated with the polymer. Since the spectra are not normalized and the peak intensity can be used for quantitative comparison, one can observe that the C–OH band at 1230 cm^{-1} is intensified at the expense of weakening the epoxy stretching band at 900 cm^{-1}. These variations in the intensities of the functional groups explicitly feature the anchoring reaction between epoxy bridges and the polymers to form hydroxyl groups. The SEM image in Fig. 2c shows the puckering feature of *p*GO, indicating that exfoliation of the graphite oxide was improved by the polymer penetration. Because the layers are not regularly stacked, we cannot observe any crystal diffraction peak in the XRD pattern of *p*GO (Fig. 1d).

Symmetric two-electrode EDLC cells were assembled for capacitive performance analysis. A schematic drawing of the EDLC cell configuration is shown in Fig. 5. The cell consists of two facing identical electrodes sandwiching a separator, which is a cellulose paper or a gel-electrolyte film. A liquid-phase electrolyte, 1 M $TEABF_4$/PC, was used to test the performance of *p*GO and a commercially available activated carbon, i.e. AC. A gel electrolyte, using P(EO-*co*-PO) as the host to entrap the 1 M $TEABF_4$/PC solution, was also incorporated with *p*GO to assemble an EDLC for examination. Fig. 6a and b shows the cyclic voltammograms recorded at varying potential sweep rates for the liquid-electrolyte cells, which used the cel-

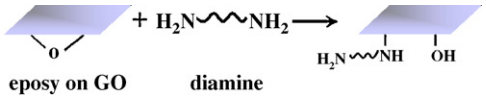

Fig. 4. Schematic representation of the anchoring reaction between the epoxy groups on graphene oxide sheets and the poly(propylene oxide) diamines to form graphene–N bonds and –OH groups.

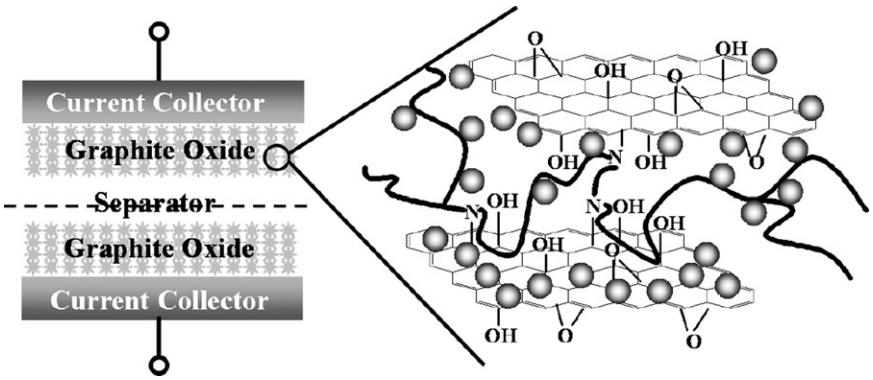

Fig. 5. Schematic of test EDLC assembly and structural model of the polymer/graphite oxide composite (*p*GO) assembled in the EDLC. The spheres in *p*GO represent the electrolyte ions, which can be conveyed via diffusion and the segmental motion of the polymer chains.

lulose paper as the separator and were soaked in the $TEABF_4$/PC electrolyte solution during measurement. Rectangular voltammograms are observed for both cells. This indicates that the profound functionalities on the graphite oxide sheets contribute a negligible amount of pseudocapacitance [11,37,38]. However, the induced current values are larger for *p*GO relative to those of AC, even if AC has a large BET surface area of 960 $m^2\,g^{-1}$. The capacitance value for *p*GO is as high as 130 $F(g\,GO)^{-1}$ at a scan rate of 5 $mV\,s^{-1}$, while that for AC is 51 $F(g\,AC)^{-1}$. The capacitance of AC would be higher if it has a larger surface area. The large capacitance for *p*GO indicates that *p*GO is conductive, as well as that polymer incorporation has promoted the transport of electrolyte ions into the interlayer space of graphite oxide.

Based on a four-point probe measurement, GO and *p*GO had electrical conductivities of 0.30 and 0.58 $S\,cm^{-1}$, respectively. We speculate that there would be some sp^2-carbon retained on the graphene oxide sheets and the vacuum-drying at 120 °C, which was conducted once for GO and twice for *p*GO, would have removed or rearranged some oxygen functionalities on the graphite oxide sheets to improve the electrical contact via partial graphitization. A vague bump near $2\theta = 25°$ appearing in the XRD patterns of GO and *p*GO (Fig. 1c and d) may indicate the occurrence of partial graphitization. A previous study showed that the conductivity of graphene oxide sheets can be significantly improved by heat treatment at temperatures as low as 125 °C [39]. The heat treatment clustered the sp^2 phase on graphene oxide sheets, forming two dimensional nanocrystalline graphene. However, other studies found that the presence of amine groups can stimulate graphitization of graphite oxide during heat treatment [22,40,41]. The detailed mechanism for the enhancement of the conductivity of *p*GO by heat treatment is not clear at this moment and much more research is required to understand all details.

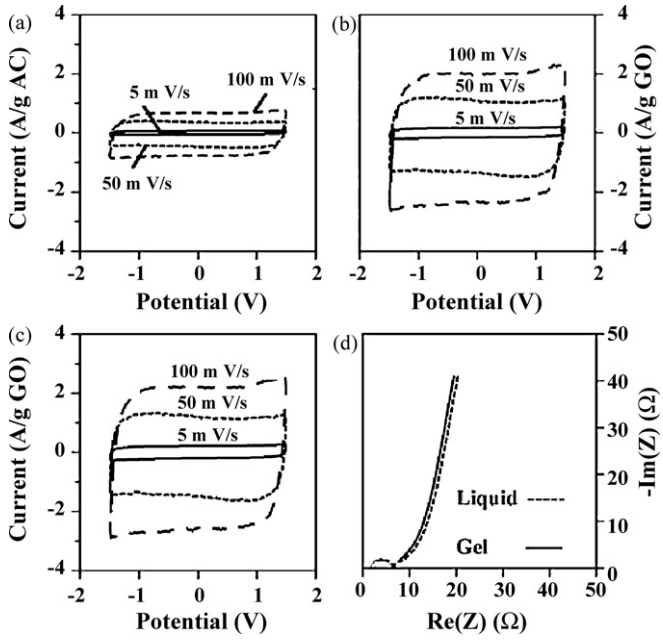

Fig. 6. Cyclic voltammograms obtained at varying scan rates of the symmetric two-electrode capacitors: (a) the cell assembled with commercial activated carbon and the organic liquid solution (1 M $TEABF_4$/PC); (b) the cell assembled with *p*GO and the organic liquid solution; (c) the "dry" cell assembled with *p*GO and the gel electrolyte. The Nyquist impedance plots of the *p*GO cells used in (b) and (c) are shown in (d).

As to the transport of electrolyte ions, a structure sketch of *p*GO is depicted in Fig. 5 to elucidate the mechanism of the intensified double layer formation on graphene oxide sheets. In the interlayer spacing of *p*GO the anchored polymer chains, which have a strong ion-solvating tendency, are responsible for the high-degree penetration of electrolyte ions (i.e. the spheres shown in Fig. 5), thereby forming a specifically adsorbed Helmholtz layer on the graphene oxide sheets, and possibly a diffuse layer [10,42].

In addition to the cellulose paper, a gel-electrolyte film was assembled with the *p*GO electrodes to form a capacitor for test under a "dry" situation. The cyclic voltammograms of the gel-electrolyte cell are shown in Fig. 6c, showing a rectangular shape to represent an excellent capacitive behavior. The current and calculated capacitance values are similar to those of the liquid-electrolyte cell assembled with *p*GO. The gel-electrolyte film must be highly compatible with the *p*GO electrodes. As a "dry" EDLC system, the capacitive performance of this gel-electrolyte cell is outstanding [20,43–50].

The variation of the capacitance values with the potential scan rate for the cells assembled with *p*GO is shown in Table 1. One can observe the decrease of capacitance with the scan rate for the two cells. The electrochemical impedance spectroscopy was used to analyze the resistance of the *p*GO-based electrodes and the results shown as Nyquist plots are depicted in Fig. 6d. The plots for both cells show a semicircle intersecting the real axis in the high frequency region, and it transforms to a vertical line with decreasing

Table 1
Specific capacitance of *p*GO assembled with liquid- and gel electrolytes at varying potential scan rates.

Potential scan rate ($mV\,s^{-1}$)	Specific capacitance ($F(g\,GO)^{-1}$)	
	Liquid electrolyte	Gel electrolyte
5	127	133
50	81	90
100	64	72

frequency. The presence of the semicircles indicates an obvious resistance for electron conduction in the electrode [51,52]. This may be due to the presence of functional groups to hinder electron conduction between the graphite oxide aggregates. We expect that a partial reduction on the *p*GO electrode can reduce the electrical resistance [53–55]. Owing to the polymer presence in *p*GO, the agglomeration of the graphene sheets obtained from reduction can hopefully be avoided [26,56]. This represents an advantage for *p*GO to have a high proportion of graphene sheets being exposed to electrolyte. Knowledge obtained from the *p*GO synthesis and application will be very useful in designing graphene-based material for versatile energy storage applications.

4. Conclusions

Polymer incorporation into graphite oxide represents a promising technology to synthesize electrode materials used in gel-electrolyte EDLC systems. The segregation of graphite oxide assures the high accessibility of graphene oxide sheets to the electrolyte ions. This is verified by the high capacitance values of *p*GO and by the double-layer feature of the capacitance with little contribution from chemical interaction. The amine functional group in the polymer plays an important role to penetrate the graphite oxide as well as to anchor the individual graphene oxide sheets. In addition, the synthesis of *p*GO was cost-effective because a high-crystallinity precursor graphite and additional chemical reduction of the resulting graphite oxide are not essentially necessary.

Acknowledgement

This research was supported by the National Science Council of Taiwan (NSC 97-2120-M-006-005).

References

[1] B.E. Conway, Electrochemical Supercapacitors: Scientific Fundamentals and Technological Applications, Plenum Publishers, New York, 1999.
[2] Y.T. Kim, T. Mitani, J. Power Sources 158 (2006) 1517–1522.
[3] J.R. Miller, P. Simon, Science 321 (2008) 651–652.
[4] E. Frackowiak, F. Béguin, Carbon 39 (2001) 937–950.
[5] R. Kötz, M. Carlen, Electrochim. Acta 45 (2000) 2483–2498.
[6] K.P. Wang, H. Teng, Carbon 44 (2006) 3218–3225.
[7] J. Chmiola, G. Yushin, Y. Gogotsi, C. Portet, P. Simon, P.L. Taberna, Science 313 (2006) 1760–1763.
[8] C. Largeot, C. Portet, J. Chmiola, P.L. Taberna, Y. Gogotsi, P. Simon, J. Am. Chem. Soc. 130 (2008) 2730–2731.
[9] J. Chmiola, C. Largeot, P.L. Taberna, P. Simon, Y. Gogotsi, Angew. Chem. Int. Ed. 47 (2008) 3392–3395.
[10] C.W. Huang, H. Teng, J. Electrochem. Soc. 155 (2008) A739–A744.
[11] D. Hulicova-Jurcakova, M. Seredych, G.Q. Lu, T.J. Bandosz, Adv. Funct. Mater. 19 (2009) 438–447.
[12] O. Barbieri, M. Hahn, A. Herzog, R. Kötz, Carbon 43 (2005) 1303–1310.
[13] H.Y. Liu, K.P. Wang, H. Teng, Carbon 43 (2005) 559–566.
[14] F. Stoeckli, T.A. Centeno, Carbon 45 (2005) 1184–1190.
[15] T.A. Centeno, F. Stoeckli, J. Power Sources 154 (2006) 314–320.
[16] H. Teng, Y.J. Chang, C.T. Hsieh, Carbon 39 (2001) 1981–1987.
[17] M.D. Stoller, S. Park, Y. Zhu, J. An, R.S. Ruoff, Nano Lett. 8 (2008) 3498–3502.
[18] Y.R. Lin, H. Teng, Carbon 41 (2003) 2865–2871.
[19] C. Sivakumar, J.N. Nian, H. Teng, J. Power Sources 144 (2005) 295–301.
[20] C.P. Tien, W.J. Liang, P.L. Kuo, H. Teng, Electrochim. Acta 53 (2008) 4505–4511.
[21] C.P. Tien, H. Teng, J. Taiwan Inst. Chem. Eng. 40 (2009) 452–456.
[22] M. Herrera-Alonso, A.A. Abdala, M.J. McAllister, I.A. Aksay, R.K. Prud'homme, Langmuir 23 (2007) 10644–10649.
[23] Y. Matsuo, K. Tahara, Y. Sugie, Carbon 35 (1997) 113–120.
[24] G. Wang, Z. Yang, X. Li, C. Li, Carbon 43 (2005) 2564–2570.
[25] S. Stankovich, D.A. Dikin, G.H.B. Dommett, K.M. Kohlhaas, E.J. Zimney, E.A. Stach, R.D. Piner, S.T. Nguyen, R.S. Ruoff, Nature 442 (2006) 282–286.
[26] S. Stankovich, D.A. Dikin, R.D. Piner, K.A. Kohlhaas, A. Kleinhammes, Y. Jia, Y. Wu, S.T. Nguyen, R.S. Ruoff, Carbon 45 (2007) 1558–1565.
[27] C. Gmez-Navarro, R.T. Weitz, A.M. Bittner, M. Scolari, A. Mews, M. Burghard, K. Kern, Nano Lett. 7 (2007) 3499–3503.
[28] D.W. Boukhvalov, M.I. Katsnelson, J. Am. Chem. Soc. 130 (2008) 10697–10701.
[29] H.K. Jeong, Y.P. Lee, R.J.W.E. Lahaye, M.H. Park, K.H. An, I.J. Kim, C.W. Yang, C.Y. Park, R.S. Ruoff, Y.H. Lee, J. Am. Chem. Soc. 130 (2008) 1362–1366.
[30] M. Toyoda, M. Inagaki, J. Phys. Chem. Solids 65 (2004) 109–117.
[31] W.S. Hummers Jr., R.E. Offeman, J. Am. Chem. Soc. 80 (1958) 1339.
[32] C.T. Hsieh, H. Teng, Carbon 40 (2002) 667–674.
[33] K.A. Trick, T.E. Saliba, Carbon 33 (1995) 1509–1515.
[34] C. Hontoria-Lucas, A.J. López-Peinado, J. de D. López-González, M.L. Rojas-Cervantes, R.M. Martín-Aranda, Carbon 33 (1995) 1585–1592.
[35] J.I. Paredes, S. Villar-Rodil, A. Martínez-Alonso, J.M.D. Tascón, Langmuir 24 (2008) 10560–10564.
[36] T. Szabó, O. Berkesi, I. Dékány, Carbon 43 (2005) 3181–3189.
[37] Y.R. Nian, H. Teng, J. Electrochem. Soc. 149 (2002) A1008–A1014.
[38] P.Z. Cheng, H. Teng, Carbon 41 (2003) 2057–2063.
[39] I. Jung, D.A. Dikin, R.D. Piner, R.S. Rouff, Nano Lett. 8 (2008) 4283–4287.
[40] Y. Matsuo, T. Miyabe, T. Fukutsuka, Y. Sugie, Carbon 45 (2007) 1005–1012.
[41] Y. Matsuo, Y. Nishino, T. Fukutsuka, Y. Sugie, Carbon 45 (2007) 1384–1390.
[42] K.P. Wang, H. Teng, J. Electrochem. Soc. 154 (2007) A993–A998.
[43] T. Osaka, X. Liu, M. Nojima, J. Power Sources 74 (1998) 122–128.
[44] T. Osaka, X. Liu, M. Nojima, T. Momma, J. Electrochem. Soc. 146 (1999) 1724–1729.
[45] H.B. Gu, J.U. Kim, H.W. Song, G.C. Park, B.K. Park, Electrochim. Acta 45 (2000) 1533–1536.
[46] R.J. Latham, S.E. Rowlands, W.S. Schlindwein, Solid State Ionics 147 (2002) 243–248.
[47] J.L. Qiao, N. Yoshimoto, M. Morita, J. Power Sources 105 (2002) 45–51.
[48] M. Morita, J.L. Qiao, N. Yoshimoto, M. Ishikawa, Electrochim. Acta 50 (2004) 837–841.
[49] C.M. Yang, W.I. Cho, J.K. Lee, H.W. Rhee, B.W. Cho, Electrochem. Solid-State Lett. 8 (2005) A91–A95.
[50] M. Morita, T. Kaigaishi, N. Yoshimoto, M. Egashira, T. Aida, Electrochem. Solid-State Lett. 9 (2006) A386–A389.
[51] J.N. Nian, H. Teng, J. Phys. Chem. B 109 (2005) 10279–10284.
[52] C.W. Huang, C.M. Chuang, J.M. Ting, H. Teng, J. Power Sources 183 (2008) 406–410.
[53] S. Stankovich, R.D. Piner, S.T. Nguyen, R.S. Ruoff, Carbon 44 (2006) 3342–3347.
[54] S. Stankovich, R.D. Piner, X. Chen, N. Wu, S.T. Nguyen, R.S. Ruoff, J. Mater. Chem. 16 (2006) 155–158.
[55] S. Gilje, S. Han, M. Wang, K.L. Wang, R.B. Kaner, Nano Lett. 7 (2007) 3394–3398.
[56] D. Li, M.B. Müller, S. Gilje, R.B. Kaner, G.G. Wallace, Nat. Nanotechnol. 3 (2008) 101–105.